Electron-pair entropic and complexity measures in atomic systems

S. López-Rosa[*], A.L. Martín[†], J. Antolín [‡], J.C. Angulo[§]

October 25, 2018

Abstract

The two-electron atomic densities are analysed in both position and momentum spaces in terms of different information-theoretic measures, such as disequilibrium, Shannon entropy, shape complexity and its corresponding information plane. This study is conveyed throughout the Periodic Table and the obtained results are discussed in terms of varied atomic properties such as (i) atomic charge, (ii) shell filling patterns and (iii) electronic correlation. A detailed discussion on how these properties modify in a particular manner the electron density structure when considering a one-electron or a two-electron density description is conducted.

[*]Departamento de Física Aplicada II, Universidad de Sevilla, 41012-Sevilla, Spain.

[†]Departamento de Física Atómica, Molecular y Nuclear, Universidad de Granada, 18071-Granada, Spain

[‡]Departamento de Física Aplicada, Universidad de Zaragoza, 50018-Zaragoza, Spain. Instituto Carlos I de Física Teórica y Computacional, Universidad de Granada, 18071-Granada, Spain

[§]Departamento de Física Atómica, Molecular y Nuclear, Universidad de Granada, 18071-Granada, Spain. Instituto Carlos I de Física Teórica y Computacional, Universidad de Granada, 18071-Granada, Spain

1 INTRODUCTION

One-electron densities have a straightforward meaning in atomic physics, as they are directly related to the probability of finding an electron in a determinate region of the atom. One can study different regions of the atomic density and thus one can understand the way electrons populating that region behave. There is a huge amount of information coded inside monoelectronic densities. However, there is some information that this kind of density lacks, mainly information about the electron correlations. These densities don't directly give us any information at all about how the position of an electron conditions the position of the others. It is in this context when electron pair densities arise[1].

Nowadays Information Theory of quantum many-body systems is attracting the attention of scientists in several fields in physical sciences, wherein major areas of research are interconnected, i.e., physics, mathematics, chemistry, and biology. It is so that there is an inherent interest for applying information-theoretic ideas and methodologies to chemical, mesoscopic and biological systems along with the processes they are involved with. In line with the aforementioned developments, multidisciplinary research projects have been undertaken so as to employ Information Theory at different levels, classical (Shannon, Fisher, complexity, etc) and quantum (von Neumann and other entanglement measures), on a variety of physical, chemical and biological systems and processes[2–4]. The Information Theory of quantum systems provides an entropy-based characterization of the atomic and molecular systems, which complements the energy-based representation obtained with the wave function and density functional methods. The physical and chemical properties of these systems can be described by means of spreading measures of entropic character of the electron density[5,6]. These measures of uncertainty, randomness, disorder and localization are basic ingredients encountered to play a relevant role for the identification and description of numerous quantum phenomena in physical systems and chemical processes.

The magnitudes of the Information Theory are very useful when trying to understand different traits and behaviours of atomic systems. There have been plenty of studies of quantum systems by means of the informational measures[7–9]. Most of these studies have been focused on the monoelectronic distributions, providing analyses on, e.g., the Shannon

entropy[10], Fisher information[11], similarity indices[12,13], different divergence measures[14,15] and complexity measures[16–18]. However, as previously mentioned, studies focused on two-electron densities require another point of view in order to analyse correlation-like qualities[19–24]. In past years there have been some successful attempts to study the electron pair densities, exposing uncertainty relationships[20], calculating information theoretical measures such as Shannon-related ones[10,21,23] or similarity measures[20,21,25,26]. This knowledge gained over the electron pair densities has translated in numerous and diverse applications. Two-electron densities have been employed to the analysis and detection of chemical bonds in molecules, finding that regions where electrons presented a higher correlations were directly related to the position of the bonds[27,28]. Electron pair densities have also been employed as a scale-down method used to study many particle systems[29–33]. Even an alternative density functional theory has been developed, with electron pair density as the functional key[1,34,35].

Some of the analyses made in the past on the electron pair density could not be as exhaustive as would have been desirable due to technical limitations of the numerical methods used, unable to calculate the two electron densities for all the atomic systems in the Periodic Table.

Preceeding studies on this subject are relatively recent[36–39], as a consequence of dealing with a subject considered some years ago, but not efficiently developed until very recently. In fact, all those publications only deal with two-electron systems, usually restricted to the analysis in terms of entropic functionals in position space. Such is the case of a pioneering work[36] regarding the information-theoretical analysis of interelectronic correlation in atomic systems, by considering a N-body density, defined from the position-space wave function $\Psi(\vec{r}_1, \ldots, \vec{r}_N)$ of the N-electron atom. Then, the functionals Fisher information I, Shannon entroy power J in terms of the Shannon entropy S, the information product $P = (IJ)/3$ and the associated information plane $I - J$ were considered, particularizing to the reduced one- and two-body densities. Other points, considered there, are: (i) the discussion of the main analytical properties regarding the aforementioned quantites (highlighting the superadditivity of I, the subadditivity of S, and the lower bound to the product P), (ii) a numerical analysis of those quantities, limited to the 6 helium-like ($N = 2$ electrons) systems with nuclear charge $Z = 1 - 5, 10$, (iii) the interpretation of the results, attending to the inter-

electronic correlation.

More recent studies afford: (i) the analysis of the four helium-like systems H^-, He, Li^+ and Ps^- (positronium negative ion)[37], attending to the dependence of the position-space Shannon entropy on the continuous variable Z (nuclear charge), particularly around the critical value for which the system becomes unstable, and posing as future work determining the momentum space entropy and checking the uncertainty relation for the total entropy $S_r + S_p \geq 3(1 + \ln \pi)$; (ii) the analysis of three Rydberg series of He doubly excited states[38], by means of Shannon entropy and Fisher information (for the reduced one-particle spatial density) and von Neumann and linear entropies (as measures of entanglement, from the reduced one-particle density matrix); and (iii) a comparative study[39] of the atomic Rényi entropies for the exponential-cosine screened Coulomb potential, by using different wave functions for the $1s^2$-state of the helium isoelectronic series.

We want to complete those studies with a more extensive list of informational quantities, using these past results as a supporting floor, and extending them to all the neutral atomic systems in the Periodic Table.

This paper is structured as follows: in the first section we show the formulation of the pair densities and how their aspect would be when used in the context of the Hartree-Fock method. The applied measures comprise the Shannon entropy, the disequilibrium and the LMC complexity, as well as the corresponding information planes. In the second section we will provide and discuss the numerical results regarding the measures showed in the previous section. Finally, some conclusions will be discussed and future works will be proposed

2 ELECTRON PAIR DENSITIES AND RELATED INFORMATION THEORETIC MEASURES

In terms of the N-electron wave function, the two-electron densities are defined as

$$\Gamma(\vec{r}_1, \vec{r}_2) = \int \Psi(\vec{x}_1, \vec{x}_2, \cdots, \vec{x}_N)\Psi^*(\vec{x}_1, \vec{x}_2, \cdots, \vec{x}_N) d\sigma_1 d\sigma_2 d\vec{x}_3 \cdots d\vec{x}_N \qquad (1)$$

in the position space, and

$$\Pi(\vec{p}_1,\vec{p}_2)=\int\Phi(\vec{y}_1,\vec{y}_2,\cdots,\vec{y}_N)\Phi^*(\vec{y}_1,\vec{y}_2,\cdots,\vec{y}_N)d\sigma_1 d\sigma_2 d\vec{y}_3\cdots d\vec{y}_N \tag{2}$$

in the momentum space. The variables $\vec{x}_i=\vec{r}_i\sigma_i$ and $\vec{y}_i=\vec{p}_i\sigma_i$ are combined coordinates which include the spin. It is well known that the physical meaning of these densities regards the probability of finding an electron with given quantum numbers within the region $\vec{r}_1 d\vec{r}_1$ if there is another electron with allowed/compatible quantum numbers within the region $\vec{r}_2 d\vec{r}_2$, and similarly regarding the momentum regions $\vec{p}_1 d\vec{p}_1$ and $\vec{p}_2 d\vec{p}_2$. These densities are directly related to the electron correlations, as the compatibility of an electron state is organically determined by the compatibility of its state with those of the others. They naturally give us quantifiers of correlation between electrons.

The two-electron densities are going to be calculated by the Hartree-Fock approach and can be expressed as follows[40]:

$$\Gamma(\vec{r}_1,\vec{r}_2)=\frac{1}{N-1}\left[N\rho(\vec{r}_1)\rho(\vec{r}_2)-\Gamma_x(\vec{r}_1,\vec{r}_2)\right] \tag{3}$$

in the position space, and

$$\Pi(\vec{p}_1,\vec{p}_2)=\frac{1}{N-1}\left[N\gamma(\vec{p}_1)\gamma(\vec{p}_2)-\Pi_x(\vec{p}_1,\vec{p}_2)\right] \tag{4}$$

in the momentum space, respectively. The functions $\rho(\vec{r_i})$ and $\gamma(\vec{p_i})$ are the one-electron densities and $\Gamma_x(\vec{r}_1,\vec{r}_2)$ and $\Pi_x(\vec{p}_1,\vec{p}_2)$ are the exchange densities in the position and momentum space respectively. Let us remark that, using Hartree-Fock functions, we are studying the Fermi correlation between same-spin electrons which arises from the antisymmetry of the wave function. In this sense, the term electron correlation, mentioned before, alludes to the statistical correlation. This point must be clarified in order to not lead to confusion if one considers a correlated system as one beyond the Hartree-Fock approximation (the Löwdin definition of correlation energy).

The Shannon entropy, S, of the normalized-to-unity electron pair densities are given by:

$$S(\Gamma)=-\int\Gamma(\vec{r}_1,\vec{r}_2)\ln\Gamma(\vec{r}_1,\vec{r}_2)d\vec{r}_1 d\vec{r}_2 \tag{5}$$

for the position space, and

$$S(\Pi)=-\int\Pi(\vec{p}_1,\vec{p}_2)\ln\Pi(\vec{p}_1,\vec{p}_2)d\vec{p}_1 d\vec{p}_2 \tag{6}$$

for the momentum space, respectively. This quantity measures the extent to which the density is spread, so that it is a measure of delocalization. Let us point out that the Shannon entropy could reach negative values. To avoid this and to guarantee that the uncertainty is non-negative, sometimes it is useful to define the exponential Shannon entropy as

$$L = e^S \tag{7}$$

Notice, in addition, that the exponential Shannon entropy is defined in this way in order to have the same dimensions as the variable considered, as the variance does, one of the most commonly used uncertainty measures.

Considering that the electron pair density is, in its spherically averaged form, bidimensional, while its corresponding monoelectronic counterpart is monodimensional, a higher value on the Shannon entropy can be expected just due to the more natural spreading of the electron pair density. The Shannon entropy has already been employed in the past for studying electron pair densities[10,20,21,26] showing how correlation effects can be successfully detected with this measure, and establishing relationships between its values and atomic properties.

The disequilibrium, self-similarity[41] or information energy[42], D, quantifies the departure from uniformity of the probability density (equiprobability). In position space, the disequilibrium for two-electron density is given by

$$D(\Gamma) = \int \Gamma^2(\vec{r}_1, \vec{r}_2) d\vec{r}_1 d\vec{r}_2, \tag{8}$$

and in momentum space is defined as

$$D(\Pi) = \int \Pi^2(\vec{p}_1, \vec{p}_2) d\vec{p}_1 d\vec{p}_2. \tag{9}$$

.

It is worthy to point out that both quantities S and D posses a global character, i.e., they consider the behavior of the distribution over its whole domain.

Aside of the properties of the entropic measures described above, it is interesting to quantify the complexity of the physical systems. The characterization of complexity is not unique and the utility of each definition depends on the type of system or process, the

level of the description, and the scale of the interactions among the constituents of the systems considered, e.g., elementary particles, atoms, molecules, biological systems, etc. Fundamental concepts such as uncertainty or randomness are frequently employed in the definitions of complexity, although some other concepts such as clustering, order, localization or organization might be also important for characterizing the complexity of systems or processes.

Here, we focus our attention on a complexity measure defined as a product of two information theoretical measures in order to simultaneously quantify two facets of the electron density of the system; namely, the *LMC shape complexity*, $C(LMC)$. This quantity was introduced in 1995 by López-Ruiz, Mancini and Calbet[43] although, later on, it has been criticized[44], modified[45,46] and generalized[47] leading to a useful estimator which reaches minimal values for both extremely ordered and disordered limits (i.e., for the Dirac-delta distribution and for the highly flat ones, respectively), satisfying also the desirable properties of invariance under scaling transformation, translation and replication[48,49]. The utility of this improved complexity has been clearly shown in many different fields[50–52] allowing reliable detection of periodic, quasiperiodic, linear stochastic and chaotic dynamics[43,48,49].

The LMC complexity is defined by the product of two single-facet entropy measures (the disequilibrium D and the exponential Shannon entropy e^S) as

$$C_{LMC}(\Gamma) = D(\Gamma) \times e^{S(\Gamma)} \tag{10}$$

in position space, and

$$C_{LMC}(\Pi) = D(\Pi) \times e^{S(\Pi)} \tag{11}$$

in momentum space. This composite information-theoretic quantity measures the complexity of the system by means of a combined balance of the average height of the probability density (as given by D) and its total bulk extent (as given by S), i.e., the uniformity and delocalization features. This quantity satisfies the bound $C_{LMC} \geq 1$ for any probabilty density, with domain of arbitrary dimensionality[53].

3 RESULTS AND DISCUSSION

In recent years, there has been an increasing interest in the information-theoretical analysis of interelectronic correlation in atomic systems. Different works have been performed within this field[36–39], nevertheless, all of them deal with two-electron systems, usually restricted to the analysis in terms of entropic functionals in position space.

This section is aimed to perform a comparative study among atomic one- and two-particle densities, on the basis of the respective information-theoretic functionals considered in the previous section. The analysis is two-fold, by considering densities in both conjugated spaces: that is, the position-space ones $\rho(\vec{r})$ and $\Gamma(\vec{r}_1, \vec{r}_2)$, and the momentum-space ones $\gamma(\vec{p})$ and $\Pi(\vec{p}_1, \vec{p}_2)$. Functions normalized to unity will be managed in what follows, for the sake of their interpretation as probability distributions.

Note that for the one-particle density, the Shannon entropy is given by

$$S(\rho) = -\int \rho(\vec{r}) \ln \rho(\vec{r}) d\vec{r}, \tag{12}$$

$$S(\gamma) = -\int \gamma(\vec{p}) \ln \gamma(\vec{p}) d\vec{p}, \tag{13}$$

in position space and momentum space, respectively.

The disequilibrium for the one-electron density in position space can be defined as

$$D(\rho) = \int \rho^2(\vec{r}) d\vec{r}, \tag{14}$$

and in momentum space is given by

$$D(\gamma) = \int \gamma^2(\vec{p}) d\vec{p}. \tag{15}$$

The LMC complesity for the one-electron density can be defined as

$$C_{LMC}(\rho) = D(\rho) \times e^{S(\rho)}, \tag{16}$$

in position space, and

$$C_{LMC}(\gamma) = D(\gamma) \times e^{S(\gamma)} \tag{17}$$

in momentum space.

Let us mention that the results for the electron-pair density have been very difficult to obtain compared to the one-electron ones, mostly due to the higher computational prowess needed to perform the calculations. Although we work with spherically averaged densities, the integration grid is still bidimensional which greatly increases the number of calculations needed to reach a required precision, i.e., if a grid with n points along a real interval is needed for the case of one-electron density, the electron-pair density will require $n^2/2$ points along a surface. In addition, calculations in momentum space require a much more extensive grid than in the position space due to the asymptotic behaviour of the densities. Computations have been performed, in both position and momentum spaces, by means of the accurate Near-Hartree-Fock wave functions of Koga et al[54,55]

3.1 Shannon entropy and disequilibrium

The electron pair density or, equivalently, two-particle density, displays fundamental differences with respect to the (more usual) one-particle distribution. Maybe one of the most remarkable distinctions regards the intrinsic uncertainty, higher in the two-particle case than in the monoelectronic one. When considering a probabilistic description based on electron pairs, instead of single particles, the result is a rise of spread. Let us remind that Shannon entropy is an appropriate uncertainty quantifier; hence, it will be used in this section to get insight about the way in which spreading is present at both one- and two-electron levels.

Let us consider the one- and two-particle densities in position space, $\rho(\vec{r})$ and $\Gamma(\vec{r}_1, \vec{r}_2)$ respectively. In Figure 1(a), the Shannon entropies $S(\rho)$ and $S(\Gamma)$ of both densities are displayed. This is done for neutral atoms with nuclear charge $Z = 2 - 103$. It is clearly observed how the curve of the electron-pair Shannon entropy $S(\Gamma)$ remains above the one-electron partner $S(\rho)$ systematically. As expected, a higher uncertainty for the two-electron density as compared to the monoelectronic one is confirmed and becomes apparent. The reason beyond that is the relationship among the joint entropy of a two-variable distribution and the entropy of the corresponding marginals for each variable.

A more detailed analysis of both curves reveals a global decreasing tendency, but not systematic. Despite such a global tendency, there appear a number of local extrema perceived as departures from the monotonic trend, being more apparent in the case of $S(\Gamma)$.

Nevertheless, the presence of many local extrema is manifest in both curves.

It is worth mentioning that the general monotonous tendencies along the respective curves of each density (ρ and Γ) as the charge increases, entail a straight interpretation attending to (i) the physical implications of such an increase of charge, and (ii) the meaning of Shannon entropy in an information-theoretical context. The just mentioned meaning was clarified in Section II, particularly by considering how this measure constitutes a quantifier of spreading or delocalization. Increasing the nuclear charge provokes a stronger attraction over the charge cloud towards the nucleus, what induces a higher concentration of the electron densities, both the one- and two-particle distributions, around their respective origins. Such effect causes a higher localization of these distributions, or equivalently, a lower delocalization, what translates into a lower value of the Shannon entropy.

Focusing on curves' structure in Figure 1(a), items to be discussed arise immediately: (i) the specific systems, as characterized by the values of Z, for which the respective local extrema appear, and (ii) a comparison between both curves attending to the number and location along them of the just mentioned extrema. Additionally, knowing the physical reasons behind those features would be particularly interesting. In order to get a deeper insight in this regard, Table 1 is shown, in which those extrema are provided, separately as maxima and minima.

From the analysis of Table 1, some global trends are worthy of being pointed out, also emphasizing some specific exceptions:

- For the entropy of the electron-pair density, $S(\Gamma)$, the set of maxima encloses the group IIA of the Periodic Table (namely alkaline earth elements). The only exception is the presence of $Z = 13$, instead of $Z = 12$ (Magnesium).

- The rest of systems that complete the above set of maxima are: $Z = 25, 43$ with a half-filled valence subshell, and $Z = 32, 50, 84$ with a p-type valence subshell.

- The minima of $S(\Gamma)$ correspond mainly to noble gases, enclosing all them with the only exception $Z = 2$ (as justified by the fact that this system is the first one within the whole set).

Notice that one should expect a null exchange density for a factorization $\Gamma(\vec{r}_1, \vec{r}_2) = \rho(\vec{r}_1)\rho(\vec{r}_2)$, corresponding to a complete absence of mutual information between both variables, as quantified by the non-negative difference $2S(\rho) - S(\Gamma) \geq 0$, and similarly for $\Pi(\vec{p}_1, \vec{p}_2)$. However, this is not true in general (due to the definition of Γ and Π as squares of determinants defined from one-electron orbitals).

- Additional minima of $S(\Gamma)$ are $Z = 24, 29, 42, 46, 79$, with similar anomalies in the shell filling pattern: a d valence subshell half-filled or completely filled, together with an inner half-filled or empty s subshell.

- A comparative analysis between the entropy of both one- and two-particle densities is in order. Despite being both of them very similar, there are some remarkable differences:

  - Some maxima of $S(\Gamma)$ do not match those of $S(\rho)$, in such a way that a given local maximum of the latter falls in a system with a neighbor which is a local maximum for the former. This happens with maxima $Z = 4, 32, 56, 88$ of $S(\Gamma)$, which respective ones for $S(\rho)$ are $Z = 3, 31, 57, 89$. Those disengagements are emphasized in Table 2, and they correspond to systems either with one or two electrons in the valence subshell ($Z = 3 - 4, 31 - 32$), or with an electron in an inner s subshell ($Z = 56 - 57, 88 - 89$).

  - These differences regarding maxima occur for some minima as well. Such is the case of systems $Z = 30, 78$ for $S(\Gamma)$, the corresponding minima of $S(\rho)$ being $Z = 29, 79$. For each pair of consecutive systems, the lightest one has a half- or completely-filled s subshell (with anomalous filling on the internal subshells), while the heavy one has an empty or full valence subshell (with anomalous filling on the internal subshells as well).

The resemblance between $S(\rho)$ and $S(\Gamma)$ is clearly appreciated in Figure 1(a), attending not only to the location of its extrema but to the range of both magnitudes as well. In Figure 1(b) we can observe the respective curves again, allowing a more accurate insight. It is apparent the extreme similarity between both curves, looking almost identical copies, just vertically shifted. Certainly, from the analysis of Figure 1 we should conclude that the only

discrepancy is a multiplicative factor, what in logarithmic scale translates into a vertical displacement of length $\log 2$. The shifted curves clearly overlap, so that we could affirm that $S(\Gamma) \approx 2S(\rho)$ for any system with $Z = 2 - 103$. It is worthy to mention that such an approximate connection between $S(\Gamma)$ and $S(\rho)$ becomes an exact equality, as a limiting case of the rigorous inequality $2S(\rho) \geq S(\Gamma)$, if the variables $(\vec{r}_1, \vec{r}_2)$ are independent. Accordingly to the previous comment, we could say that the electron spatial locations are 'roughly' independent, at least in atomic systems. In terms of mutual information, the previous comment translates into negligible values of the atomic mutual information. Nevertheless, efficient comparative functionals between Γ and ρ will be suggested in the concluding section, in order to study more in detail and to explain the above fact.

In Figure 2, Shannon entropy of one-electron and electron pair densities in momentum space is displayed, for neutral atoms with nuclear charge $Z = 2-103$. As previously observed in position space: (i) the Shannon entropy values of the two-electron density are much higher than those of the one-electron density; and (ii) an almost perfect overlap between one- and two-electron entropies occurs when comparing the momentum space values $2S(\gamma)$ and $S(\Pi)$. In momentum space, no complex structure is observed, but just a monotonic increase, more apparent in the low-Z region, and even more for the pair density. For higher values of Z the increase becomes softer. This fact deserves to be interpreted in depth by means of 'mutual information', by comparing the global behaviors and structures along both conjugated spaces. The authors will provide a detailed analysis in a near future.

It is well known that Shannon entropy fulfils the entropic uncertainty relation[56]

$$S(\rho) + S(\Gamma) \geq 3\,(1 + \ln \pi)\,, \tag{18}$$

while for the two-electron densities, this uncertainty-type entropic relation becomes[26]:

$$S(\gamma) + S(\Pi) \geq 6\,(1 + \ln \pi)\,. \tag{19}$$

In Figure 3, the Shannon entropy sums for one- and two-electron densities have been depicted. The respective curves display similar paths, roughly shifted by a constant factor (an exact shift would occur in case of dealing with pairs of independent variables).

Let us now pay attention to the disequilibrium of one-electron and electron pair densities, particularly in position space, as depicted in Figure 4 for atomic systems with nuclear charge

$Z = 2-103$. It is observed in the figure that, for both densities, the disequilibrium increases with increasing nuclear charge, as expected. This is due to the higher nuclear attraction over the electron cloud: a higher localization around the origin occurs in position space (revealed by a decrease of Shannon entropy and an increase of disequilibrium), and a higher delocalization in momentum space (with an overall increase of the momentum range). In the low-Z region, a remarkable growth can be appreciated for the one-electron density, even more than for the two-electron density. The most remarkable trait is how the curves intersect around $Z = 10$. For very light systems, with low nuclear charge, the disequilibrium for the electron pair density is below that of the one-electron density. This is due to the low amount of electron pairs for systems with such a low number of electrons, what reduces the effect of contraction provoked by the nucleus. This occurrence, along with the knowledge that disequilibrium quantifies the relative strength of the nuclear attraction towards the electron cloud, is a measure of the exact point where the electron interaction significantly reduces the effect of the nuclear contraction. For higher values of Z the opposite occurs, what results in a higher disequilibrium value.

Regarding the conjugate space, we can see in Figure 5 the disequilibrium of the above densities in momentum space, and how they display identical structure of extrema, and roughly the same monotonic tendencies as the Shannon entropy in position space (see Figure 1). In this space, both curves do not intersect, being the value of disequilibrium of one-electron density higher than the two-electron ones for all nuclear charge Z.

3.2 LMC shape complexity

After analysing the Shannon entropy and the disequilibrium, we are in position to obtain the LMC complexity measures, given by Eqs. (10) and (11) for the one- and two-electron densities, respectively. In Figure 6, the LMC complexity measure of the aforementioned densities is depicted for atomic systems with nuclear charge $Z = 2 - 103$, in position and momentum spaces. A detailed discussion on the one-electron case can be found in Ref.[17].

Regarding the two-electron case in position space, numerous local extrema appear in Figure 6(a), matching those of the Shannon entropy S previously discussed. This is due to the fact that the exponential entropy is the dominant factor for the LMC complexity

in the present case, what defines its structure of extrema. However, the LMC value is much higher than the S one, due to (i) the exponentiation of the Shannon entropy, and (ii) the presence of the disequilibrium which acts as a modulator, so increasing even more the complexity value for higher Z. As compared to the one-electron case, the set of minima exhibited by the electron pair density presents a similar structure, as both display local minima at $Z = 10, 18, 24, 36, 42, 46$, (i.e. noble gases and anomalous shell-filling systems). The structure of maxima, however, is slightly different.

In momentum space the discussion is roughly the same, but now the extrema along the LMC curve in Figure 6(b) are those appearing in the disequilibrium, as the Shannon entropy in momentum space has barely any structure, the extrema being modulated by the Shannon entropy value, so causing a general increasing tendency.

Previous comments about the LMC complexity measure can be also induced from the corresponding information plane in Figure 7, subtended by the constituent factors D and L. In Figure 7(a), the information plane $D - L$ in position space is shown for monoelectronic and electron pair densities. The respective curves display similar structures regarding the appearance of local extrema, and a global difference is perceived in the form of a shifting constant factor. The analogous plane $D^2 - L^2$, conformed by the square of those quantities for the monoelectronic density, has been depicted in Figure 7(b). It displays a structure similar to the previous one; however, one- and two-electron curves become closer. Notice that a perfect overlap would occur in case of a factorization $\Gamma(\vec{r}_1, \vec{r}_2) = \rho(\vec{r}_1)\rho(\vec{r}_2)$, as obtained for independent variables. So, deviations from the overlap quantify the mutual information between the spatial variables $\vec{r}_1$ and $\vec{r}_2$ or, equivalently, the electron correlation. Let us mention that the information plane $D - L$ in momentum space provides similar information as the position space one. This is due to the existence of an unstructured factor and a structured one (D or L, depending on the space considered), but with similar paths along the corresponding plane, and also similar values and structure of the products DL in both spaces.

4 CONCLUSIONS

In this work, a variety of informational measures has been employed in order to perform a comparative study among atomic one- and two-particle densities. The aim of this analysis is to better understand the differences between these densities. The information measures employed for this purpose comprise Shannon entropy, disequilibrium and the LMC complexity measure.

The Shannon entropy has been calculated for the one-electron and electron-pair densities in both position and momentum spaces. In position space we found a high resemblance between both quantities, with a similar extrema structure but a higher value for the two-particle densities. As expected, a higher uncertainty for the electron-pair density as compared to the one-electron ones is confirmed. The analysis of their extrema structure has been carried out in detail. Thus, the Shannon entropy has proved its success when quantifying electronic configuration properties when applied to the electron-pair densities, providing even more sensibility to these qualities due to its higher value when compared with its one-electron alternative. It is worth mentioning that the resulting curves overlap, $S(\Gamma) \sim 2S(\rho)$, so that the electron spatial locations are roughly independent, at least in the atomic case. In momentum space, the resemblance was considerable as well, although in both one- and two-electron levels there is bare structure, just a monotonous increase. In this space, the overlap between both curves also occurs. We can say that the monoelectronic and electron pair Shannon entropies behave very similarly in position and momentum spaces and that, in terms of spreading and delocalization, both one- and two-electron densities behave in an analogous manner in both position and momentum spaces.

The disequilibrium has been quantified in a comparable way for both kind of densities in both conjugated spaces. In position space, it showed an structure-free monotonous type of behaviour, much akin to Shannon entropy in momentum space. Even so, a relevant difference could be observed: the curves for one-electron and electron-pair densities intersect around $Z = 10$. For very light systems, the disequilibrium for the two-particle density is below that of the one-electron density. This is due to the low amount of electron pairs which reduces the effect of contraction provoked by the nucleus. This occurrence, along with the knowledge that

disequilibrium quantifies the relative strength of the nuclear attraction towards the electron cloud, is a measure of the exact point where the electron interaction significantly reduces the effect of the nuclear contraction. In momentum space, the disequilibrium displays identical structure of extrema, and roughly the same monotonic behavior as the Shannon entropy in position space.

The LMC complexity in position space showed the same structure as the Shannon entropy, i.e., the same extrema structure, which means that the exponential entropy is the dominant factor for the LMC complexity. The spreading effect affects the electron-pair densities in a more relevant way as the nuclear contraction. Considering the electronic interaction mentioned above and how it affected the disequilibrium, the Shannon-dominated LMC is another proof of the more predominant effect of the electron interaction in the two-electron density when compared with the one-electron density. This change to the opposite situation in the momentum space, where the disequilibrium causes the appearance of extrema and Shannon entropy just modulates the structure.

We can conclude that information theoretical measures have been proved successful when employed to quantify electron-pair densities characteristics. It has been proved the well-known existing dissimilarities between one-electron and two-electron densities. Some previous studies, performed by other authors[21,23], have been extended to new systems, confirming known tendencies and finding new ones.

Research lines for future work include the definition of information measures based on the exchange densities, Eqs. (3) and (4), or the analysis of direct comparative functionals between the monoelectronic and the electron pair densities. So, it is expected to go beyond the actual results, based on the comparison of the results provided by each funtional at both the one- and two-electron levels, namely $F(\rho)$ and $F(\Gamma)$. Instead, one could consider quantifiers $F(\Gamma, \rho)$ of dissimilarity or divergence which, in fact, would quantify electron correlation or mutual information in case of being non-negative, and vanishing only for independent variables.

ACKNOWLEDGMENTS

This work was supported in part by the Spanish MINECO project FIS2014-59311-P (co-financed by FEDER), and the grants FQM-4643 and FQM-7276 of Junta de Andalucía. A.L.M., J.C.A. and J.A. belong to the Andalusian research group FQM-020, and S.L.R. to FQM-239.

References

1. P. W. Ayers and M. Levy, J. Chem. Science **117**, 507 (2005).

2. R. A. Gatenby and B. R. Frieden, Bull. Math. Bio. **69**, 635 (2007).

3. R. O. Esquivel, J. C. Angulo, J. S. Dehesa, J. Antolín, S. López-Rosa, N. Flores-Gallegos, M. Molina-Espíritu, and C. Iuga, *Information Theory: New Research* (Nova Science Publisher, New York, 2012), chap. Recent Advances Toward the Nascent Science of Quantum Information Chemistry.

4. M. Portesi, F. Holik, P. W. Lamberti, G. M. Bosyk, G. Bellomo, and S. Zozor, Eur. Phys. J. (2017), accepted.

5. B. R. Frieden, *Science from Fisher Information* (Cambridge University Press, Cambridge, 2004).

6. J. S. Dehesa, S. López-Rosa, and D. Manzano, in *Statistical Complexities: Applications in Electronic Structures*, edited by K. D. Sen (Springer, Berlin, 2010).

7. G. M. Bosyk, G. Bellomo, S. Zozor, M. Portesi, and P. W. Lamberti, Physica A **462**, 930 (2016).

8. R. F. Nalewajski, *Information Theory of Molecular Systems* (Elsevier, Amsterdam, 2016).

9. P. W. Lamberti, M. T. Martin, A. Plastino, and O. A. Rosso, Physica A **334**, 119 (2004).

10. N. L. Guevara, R. P. Sagar, and R. O. Esquivel, Phys. Rev. A **67** (2003).

11. A. Borgoo, P. Geerlings, and K. D. Sen, Phys. Lett. A **372**, 5106 (2008).

12. J. Antolín and J. C. Angulo, Eur. Phys. J. D. **46**, 21 (2008).

13. J. C. Angulo and J. Antolín, J. Chem. Phys. **126**, 044106 (2007).

14. J. Antolín, J. C. Angulo, and S. López-Rosa, J. Chem. Phys. **130**, 074110 (2009).

15. S. López-Rosa, J. Antolín, J. C. Angulo, and R. O. Esquivel, Phys. Rev. A **80**, 012505 (2009).

16. J. C. Angulo and J. Antolín, J. Chem. Phys. **128**, 164109 (2008).

17. J. C. Angulo, J. Antolín, and K. D. Sen, Phys. Lett. A **372**, 670 (2008).

18. J. Antolín and J. C. Angulo, Int. J. Quant. Chem. **109**, 586 (2009).

19. K. E. Banyard and J. C. Moore, J. Phys. B: At. Mol. Opt. **10**, 2781 (1977).

20. N. L. Guevara, R. P. Sagar, and R. O. Esquivel, J. Chem. Phys. **122**, 084101 (2005).

21. R. P. Sagar and N. L. Guevara, J. Chem. Phys. **123**, 044108 (2005).

22. R. Ponec and M. Strnad, J. Chem. Inf. Comput. Science **32**, 693 (1992).

23. R. P. Sagar, H. G. Laguna, and N. L. Guevara, Chem. Phys. Lett. **514**, 352 (2011).

24. H. T. Peng and Y. K. Ho, Entropy **17**, 1882 (2015).

25. X. Fradera, M. Duran, and J. Mestres, Theor. Chem. Acc **99**, 44 (1998).

26. N. L. Guevara, R. P. Sagar, and R. O. Esquivel, J. Chem. Phys. **119**, 7030 (2003).

27. R. F. W. Bader and M. E. Stephens, J. Amer. Chem. Soc. **97**, 7391 (1975).

28. M. Kohout, Faraday Discuss. **135**, 43 (2007).

29. E. R. Davidson, Chem. Phys. Lett. **246**, 209 (1995).

30. A. J. Coleman, E. P. Yukalova, and V. I. Yukalov, Int. J. Quant. Chem. **54**, 211 (1995).

31. S. K. Samvelyan, Int. J. Quant. Chem. **65**, 127 (1997).

32. M. E. Pistol, Chem. Phys. Lett. **400**, 548 (2004).

33. P. W. Ayers and E. R. Davidson, Int. J. Quant. Chem. **1006**, 1487 (2006).

34. P. Ziesche, Int. J. Quant. Chem. **60**, 1361 (1996).

35. M. Levy and P. Ziesche, J. Chem. Phys. **115**, 9110 (2001).

36. E. Romera and J. S. Dehesa, J. Chem. Phys. **120**, 8906 (2004).

37. C. Lin and Y. Ho, Chem. Phys. Lett. **633**, 261 (2015).

38. J. P. Restrepo Cuartas and J. L. SanzVicario, Phys. Rev. A **91**, 052301 (2015).

39. I. Nasser, M. Zeama, and A. Abdel-Hady, Result. Phys. **7**, 3892 (2017).

40. P. O. Löwdin, Phys. Rev. **97**, 1474 (1955).

41. R. Carbó, L. Lleyda, and M. Arnau, Int. J. Quant. Chem. **17**, 1185 (1980).

42. O. Onicescu, C.R. Acad. Sci. Paris A **263**, 25 (1966).

43. R. López-Ruiz, H. L. Mancini, and X. Calbet, Phys. Lett. A **209**, 321 (1995).

44. C. Anteneodo and A. R. Plastino, Phys. Lett. A **223**, 348 (1996).

45. R. G. Catalan, J. Garay, and R. López-Ruiz, Phys. Rev. E **66**, 011102 (2002).

46. M. T. Martin, A. Plastino, and O. A. Rosso, Phys. Lett. A **311**, 126 (2003).

47. R. López-Ruiz, Biophys. Chem. **115**, 215 (2005).

48. T. Yamano, Physica A **340**, 131 (2004).

49. T. Yamano, J. Math. Phys. **45**, 1974 (2004).

50. O. A. Rosso, M. T. Martin, and A. Plastino, Physica A **320**, 497 (2003).

51. K. C. Chatzisavvas, C. C. Moustakidis, and C. P. Panos, J. Chem. Phys. **123**, 174111 (2005).

52. A. Borgoo, F. De Proft, P. Geerlings, and K. D. Sen, Chem. Phys. Lett. **444**, 186 (2007).

53. S. López-Rosa, J. C. Angulo, and J. Antolín, Physica A **388**, 2081 (2009).

54. T. Koga, K. Kanayama, S. Watanabe, and A. J. Thakkar, Int. J. Quant. Chem. **71**, 491 (1999).

55. T. Koga, K. Kanayama, S. Watanabe, T. Imai, and A. J. Thakkar, Theor. Chem. Acc. **104**, 411 (2000).

56. I. Bialynicki-Birula and J. Mycielski, Commun. Math. Phys. **44**, 129 (1975).

Figure 1: Shannon entropy in position space of the monoelectronic and the electron pair density, $S(\rho)$ and $S(\Gamma)$ respectively, for neutral atoms with $Z = 2 - 103$; (a) $S(\rho)$ and $S(\Gamma)$ vs. Z, (b) $2S(\rho)$ and $S(\Gamma)$ vs. Z. Atomic units (a.u.) are used.

Figure 2: Shannon entropy in momentum space of the monoelectronic and the electron pair density, $S(\gamma)$ and $S(\Pi)$ respectively, for neutral atoms with $Z = 2 - 103$; (a) $S(\gamma)$ and $S(\Pi)$ vs. Z, (b) $2S(\gamma)$ and $S(\Pi)$ vs. Z. Atomic units (a.u.) are used.

Figure 3: Shannon entropy sum of the monoelectronic, $S(\rho) + S(\gamma)$, and the electron pair density $S(\Gamma) + S(\Pi)$, for neutral atoms with $Z = 2 - 103$. Atomic units (a.u.) are used.

Figure 4: Disequilibrium for monoelectronic and electron pair densities, $D(\rho)$ and $D(\Gamma)$ respectively, in position space for atomic system with $Z = 2 - 103$. Atomic units (a.u.) are used.

Figure 5: Disequilibrium for monoelectronic and electron pair densities, $D(\gamma)$ and $D(\Pi)$ respectively, in momentum space for atomic system with $Z = 2 - 103$. Atomic units (a.u.) are used.

Figure 6: LMC complexity (C_{LMC}) of the one-electron and the electron-pair densities, in (a) position and (b) momentum spaces, for systems with nuclear charge $Z = 2 - 103$, in logarithmic scale.

Figure 7: Disequilibrium-Shannon information plane, (a) $D - L$ plane for monoelectronic and electron pair densities, (b) $D^2 - L^2$ plane for monoelectronic densities and $D - L$ for electron pair densities. Atomic units (a.u.) are used.

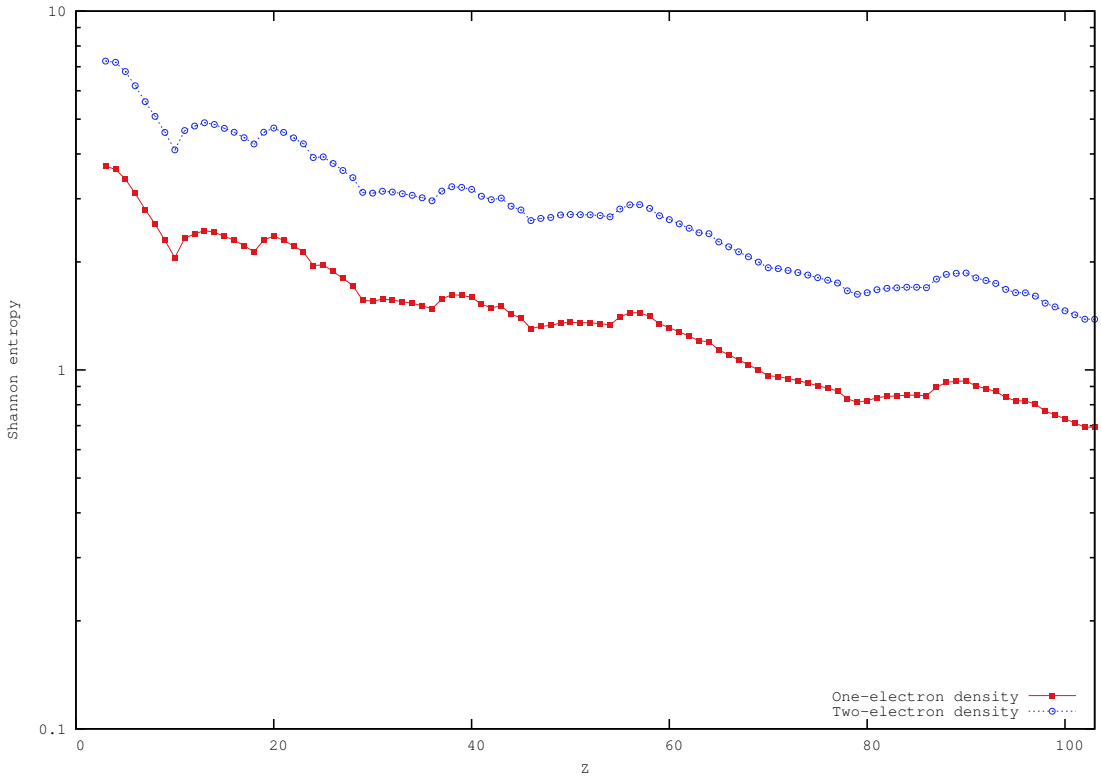

Figure 1a
S. López-Rosa, A.L. Martín, J. Antolín, J.C. Angulo
Int. J. Quant. Chem.

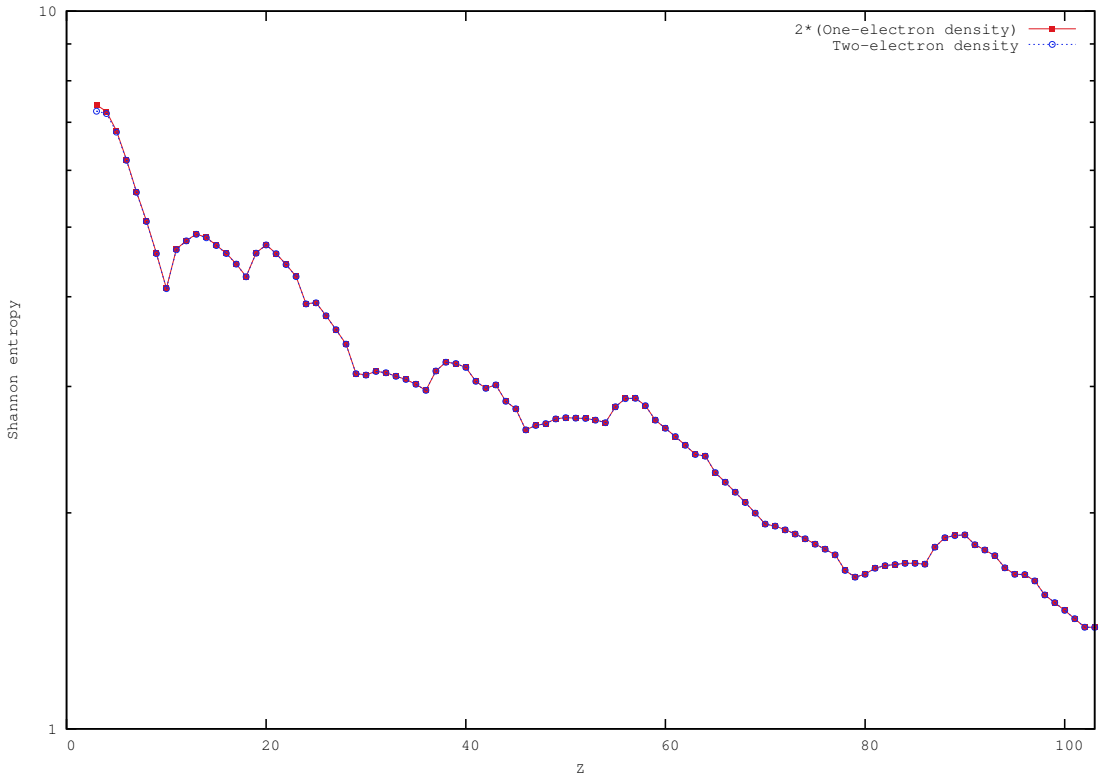

Figure 1b
S. López-Rosa, A.L. Martín, J. Antolín, J.C. Angulo
Int. J. Quant. Chem.

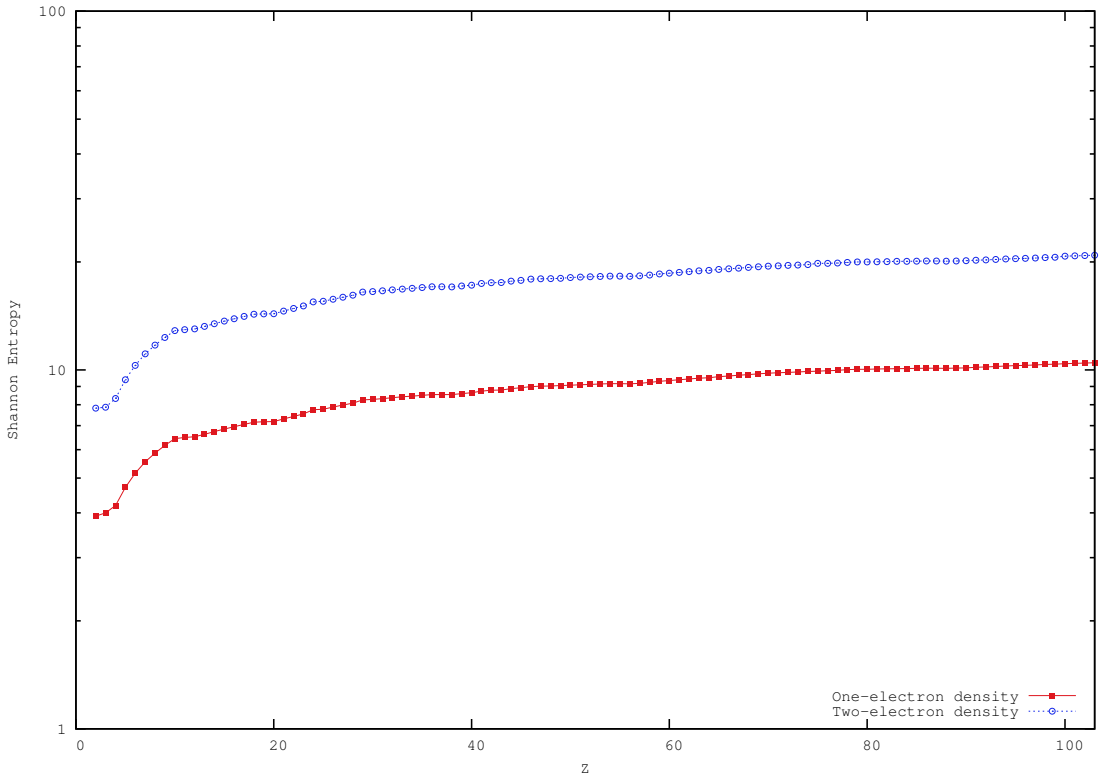

Figure 2a
S. López-Rosa, A.L. Martín, J. Antolín, J.C. Angulo
Int. J. Quant. Chem.

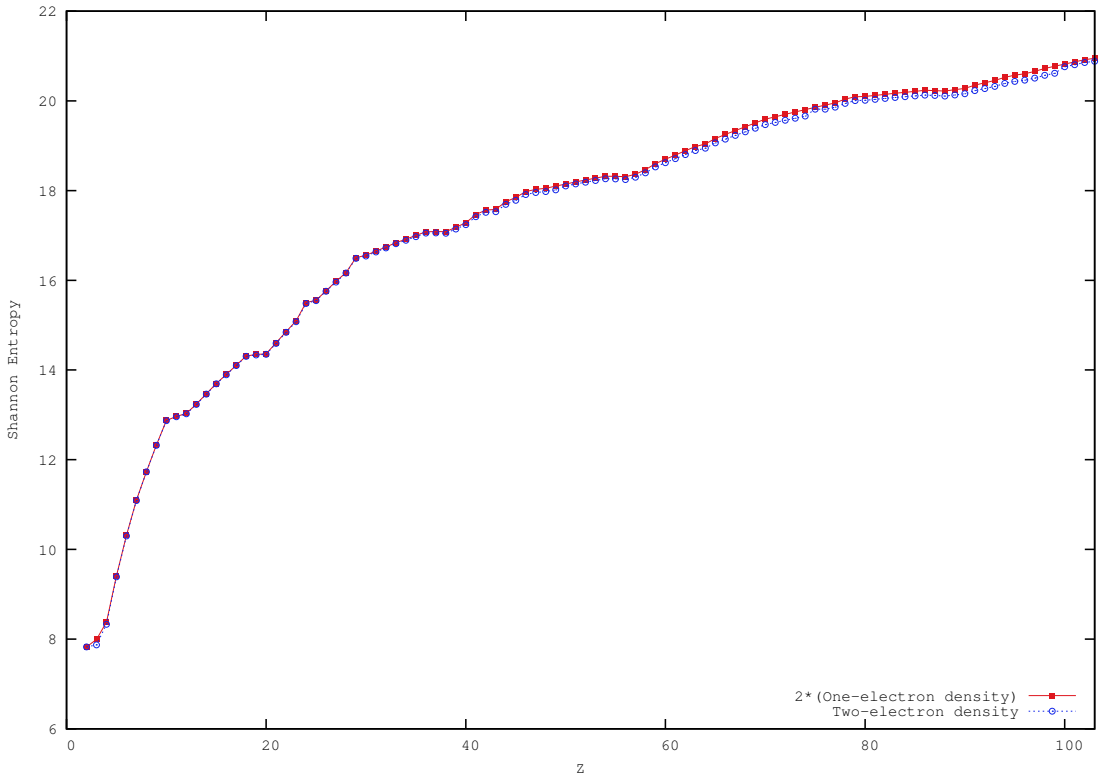

Figure 2b
S. López-Rosa, A.L. Martín, J. Antolín, J.C. Angulo
Int. J. Quant. Chem.

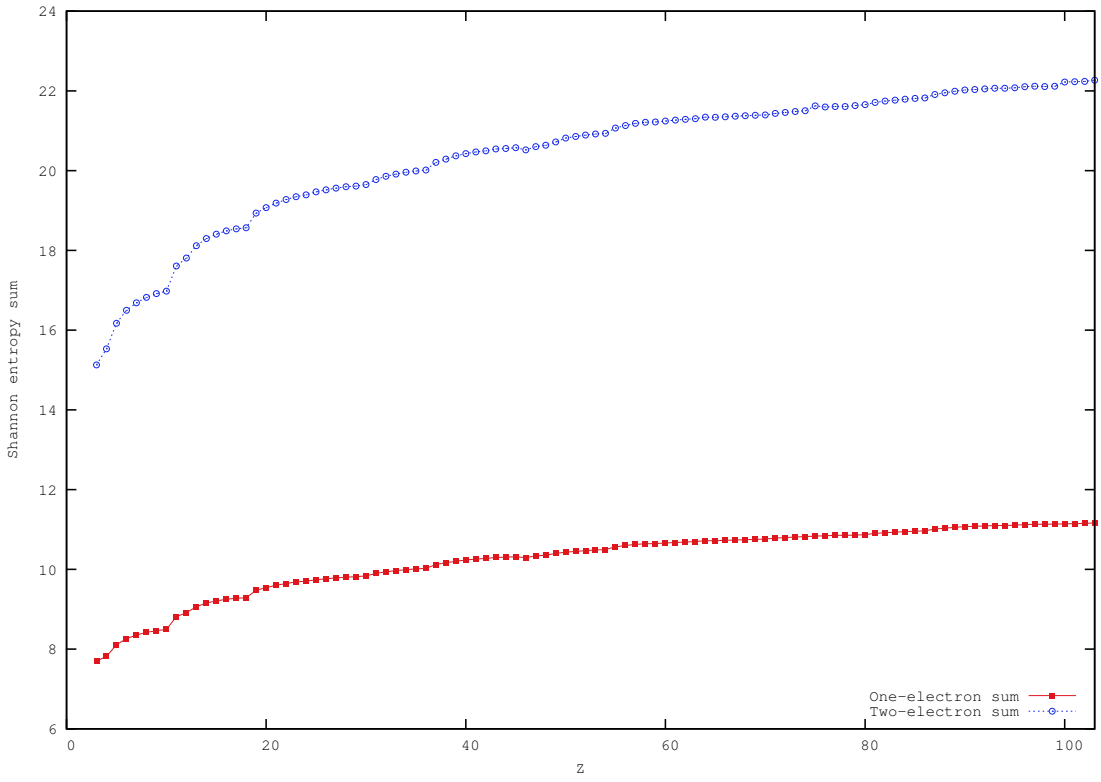

Figure 3
S. López-Rosa, A.L. Martín, J. Antolín, J.C. Angulo
Int. J. Quant. Chem.

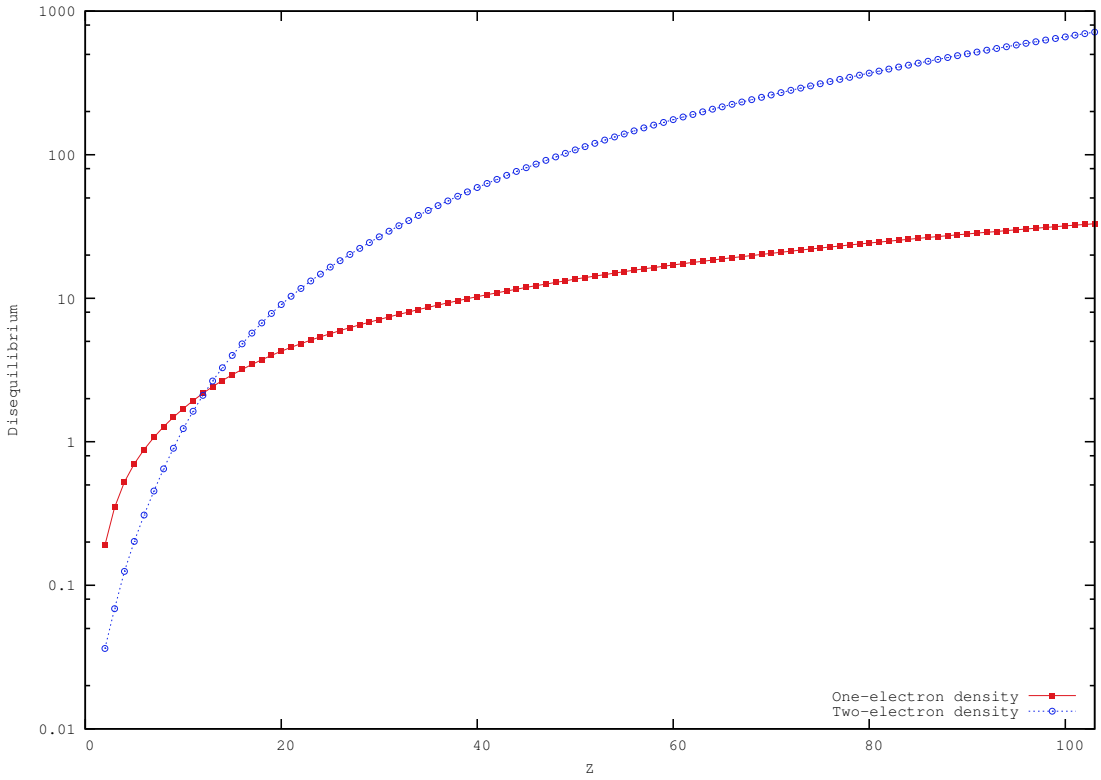

Figure 4
S. López-Rosa, A.L. Martín, J. Antolín, J.C. Angulo
Int. J. Quant. Chem.

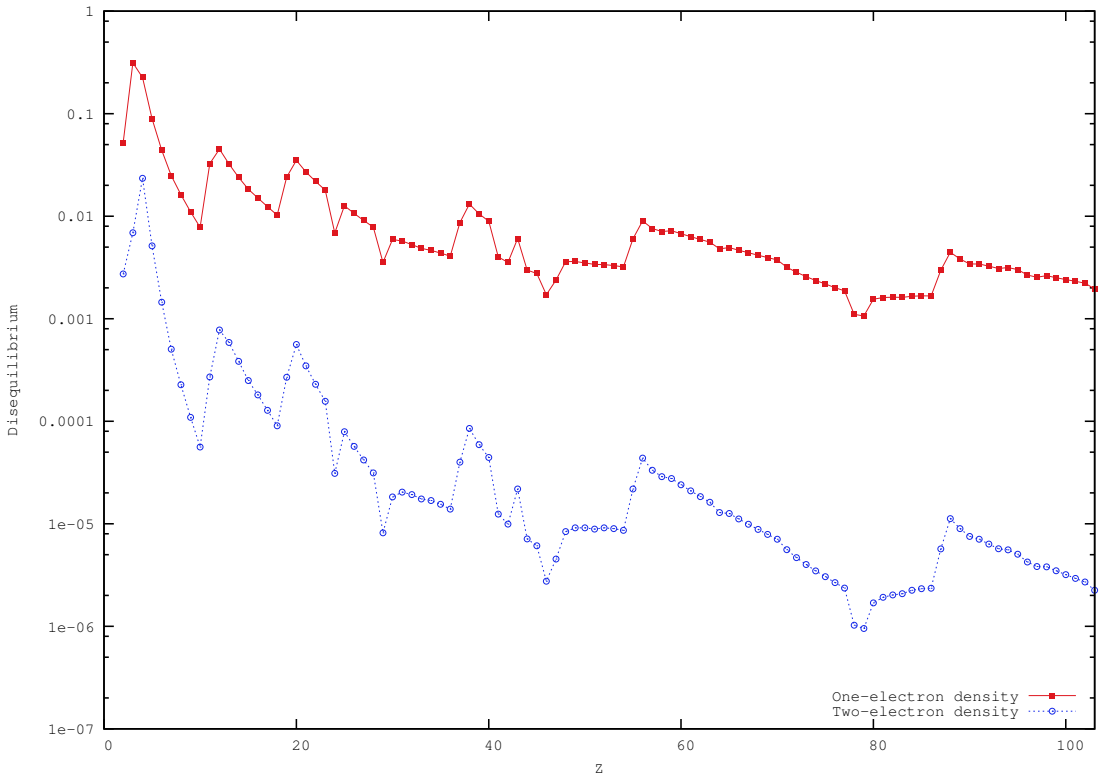

Figure 5
S. López-Rosa, A.L. Martín, J. Antolín, J.C. Angulo
Int. J. Quant. Chem.

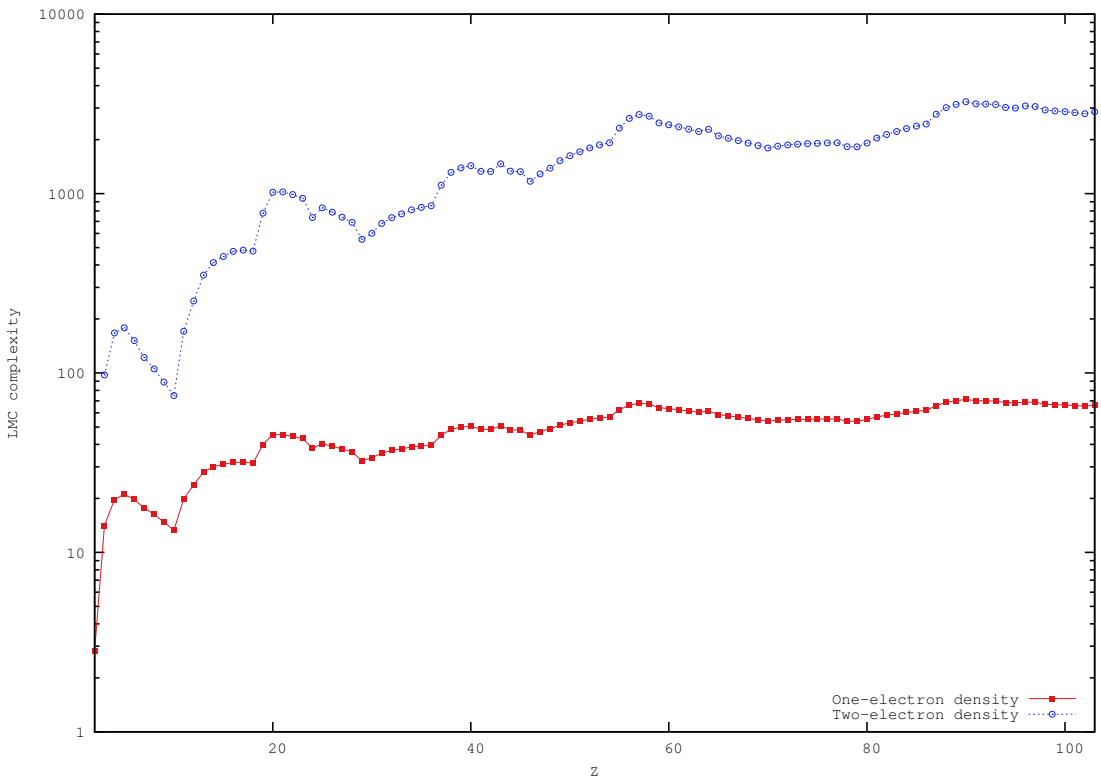

Figure 6a
S. López-Rosa, A.L. Martín, J. Antolín, J.C. Angulo
Int. J. Quant. Chem.

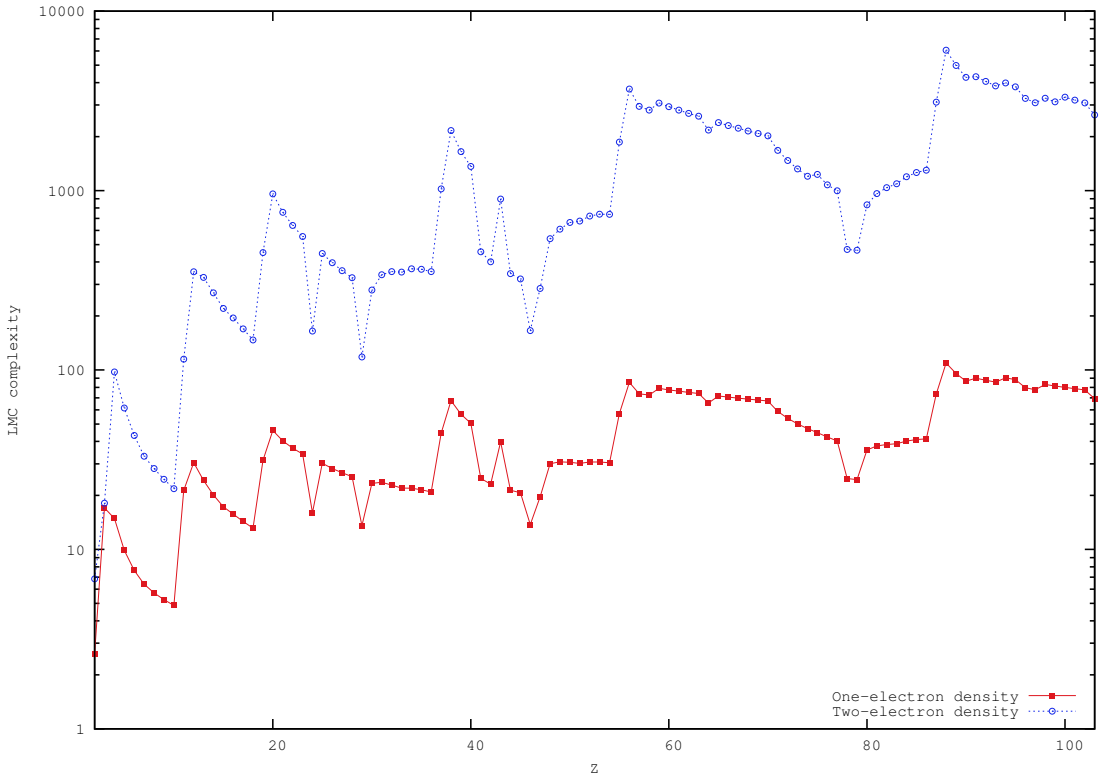

Figure 6b
S. López-Rosa, A.L. Martín, J. Antolín, J.C. Angulo
Int. J. Quant. Chem.

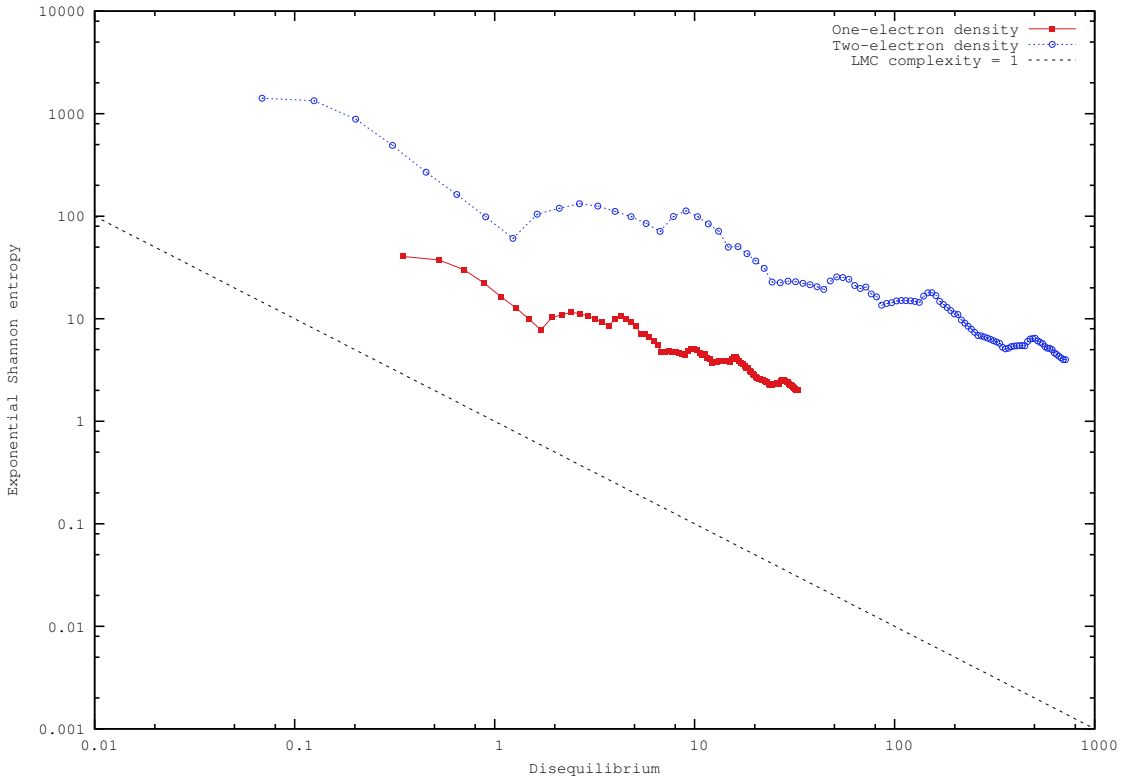

Figure 7a
S. López-Rosa, A.L. Martín, J. Antolín, J.C. Angulo
Int. J. Quant. Chem.

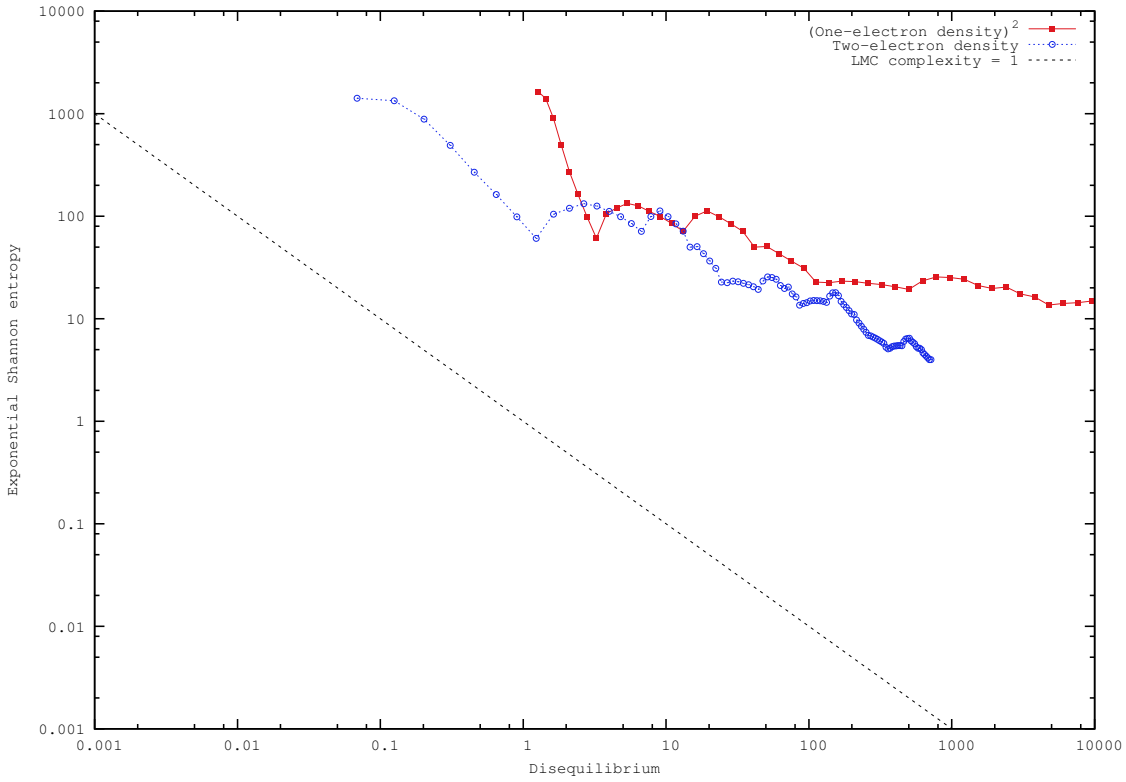

Figure 7b
S. López-Rosa, A.L. Martín, J. Antolín, J.C. Angulo
Int. J. Quant. Chem.

Maxima		**Minima**	
$\mathbf{S}(\rho)$	$\mathbf{S}(\mathbf{\Gamma})$	$\mathbf{S}(\rho)$	$\mathbf{S}(\mathbf{\Gamma})$
3	4		
13	13	10	10
20	20	18	18
25	25	24	24
31	32	30	29
38	38	36	36
	43		42
50	50	46	46
57	56	54	54
84	84	78	79
89	88	86	86

Table 1: Local extrema of position-space one- and two-particle Shannon entropies, $S(\rho)$ and $S(\Gamma)$ respectively, for neutral atoms with nuclear charge $Z = 2 - 103$. Atomic units (a.u.) are used.

Maxima			Minima		
System		Valence subshell	System		Valence subshell
3	Li	$2s^1$	10	Ne	$2p^6$
4	Be	$2s^2$	18	Ar	$3p^6$
13	Al	$3p^1$	24	Cr	$4s^1 3d^5$
20	Ca	$4s^2$	29	Cu	$4s^1 3d^{10}$
25	Mn	$3d^5$	30	Zn	$4s^2 3d^{10}$
31	Ga	$4p^1$	36	Kr	$4p^6$
32	Ge	$4p^2$	42	Mo	$5s^1 4d^5$
38	Sr	$5s^2$	46	Pd	$5s^0 4d^{10}$
43	Tc	$4d^5$	54	Xe	$5p^6$
50	Sn	$5p^2$	78	Pt	$6s^1 5d^9$
56	Ba	$6s^2$	79	Au	$6s^1 5d^{10}$
57	La	$6s^2 5d^1$	86	Rn	$6p^6$
84	Po	$6p^4$			
88	Ra	$7s^2$			
89	Ac	$7s^2 6d^1$			

Table 2: Valence subshell of systems corresponding to the local extrema of Shannon entropy in position space.